AD/A-006 978

DEVELOPMENT OF IR TRANSMITTING CHALCOGENIDE WINDOWS

Cornelius T. Moynihan, et al

Catholic University of America

Prepared for:

Office of Naval Research
Advanced Research Projects Agency

February 1975

DEVELOPMENT OF IR TRANSMITTING CHALCOGENIDE GLASSES

by

C.T. Moynihan, P.B. Macedo, M.S. Maklad,
R.K. Mohr, R.E. Howard, and P.S. Danielson

Vitreous State Laboratory
Catholic University of America
Washington, DC 20064

Final Technical Report

February, 1975

Sponsored by Advanced Research Projects Agency
ARPA Order No. 2138

Monitored by Office of Naval Research
Contract No. N00014-67-A-0377-0017
Program Code No. 4D10

Contract Period: 1 April 1972 to 30 September 1974

Amount of Contract: $273,249

Principal Investigators and Phone Numbers:
P.B. Macedo 202-635-5327
C.T. Moynihan 202-635-5180

Scientific Officer: Director, Metallurgy Program
Office of Naval Research
Department of the Navy
Arlington, VA 22217

The views and conclusions contained in this document are those of the authors and should not be interpreted as necessarily representing the official policies, either expressed or implied, of the Advanced Research Projects Agency or the U.S. Government.

Security Classification

DOCUMENT CONTROL DATA - R & D

(Security classification of title, body of abstract and indexing annotation must be entered when the overall report is classified)

1. ORIGINATING ACTIVITY (Corporate author)
Vitreous State Laboratory
Catholic University of America
Washington, DC 20064

2a. REPORT SECURITY CLASSIFICATION
Unclassified

2b. GROUP

3. REPORT TITLE
Development of IR Transmitting Chalcogenide Windows

4. DESCRIPTIVE NOTES *(Type of report and inclusive dates)*
Final Technical Report, 1 April 1972 to 30 September 1974

5. AUTHOR(S) *(First name, middle initial, last name)*
Cornelius T. Moynihan, Pedro B. Macedo, Mohktar S. Maklad, Robert K. Mohr, Regan E. Howard and Paul S. Danielson

6. REPORT DATE	7a. TOTAL NO. OF PAGES	7b. NO. OF REFS
February 1975	38	42

8a. CONTRACT OR GRANT NO.
N000014-67-A-0377-0017

b. PROJECT NO.
ARPA Order No. 2138

c. Program Code No. 4D10

d.

9a. ORIGINATOR'S REPORT NUMBER(S)

9b. OTHER REPORT NO(S) *(Any other numbers that may be assigned this report)*

10. DISTRIBUTION STATEMENT

11. SUPPLEMENTARY NOTES

12. SPONSORING MILITARY ACTIVITY
Advanced Research Projects Agency

13. ABSTRACT

A quantitative study of infrared absorption in the 250-4000cm^{-1} region of As_2Se_3 glasses doped with small amounts of As_2O_3 or purified by various procedures has been carried out with particular attention to absorption in the wavelength regions of the CO_2 and CO lasers. The dependence of the relative intensities of the oxide impurity bands in the 650-1340cm^{-1} region on the total amount of As_2O_3 added to the glass indicates the existence of three distinct oxide impurity species. A number of higher frequency impurity bands which are due to the presence of hydrogen in the glass and whose intensities are highly dependent on the glass melting conditions have been observed and classified. Absorption coefficients of As_2Se_3glass in the 920-1090 cm^{-1} CO_2 laser region are limited by intrinsic multiphonon absorption to values of around 10^{-2}cm^{-1}. The lowest absorption coefficients measured in the 1700-2000 cm^{-1} CO laser region were around 2×10^{-3} cm^{-1} and may contain contributions from hydrogen impurity bands.

Intrinsic multiphonon absorption coefficients of mixed As_2Se_3-$GeSe_2$ glasses were found to be of the same magnitude at the same respective frequencies as those for pure As_2Se_3 glass. Hence selenide glasses are unsuitable as windows for high power CO_2 lasers. (Cont'd on sep. p.)

DD FORM 1 NOV 65 1473

PRICES SUBJECT TO CHANGE

Security Classification

ABSTRACT continued

The "molecular model" of Lucovsky and coworkers for vibrational properties of chalcogenide glasses such as As_2S_3, As_2Se_3, GeS_2 and $GeSe_2$ suggests that multiphonon absorption in these materials should be analogous to overtone and combination vibrational bands in isolated molecules. A variety of experiments have been carried out whose results are in reasonable accord with this prediction. These include Raman spectra of As_2S_3 glass, measurement of the frequency dependence of infrared absorption in the multiphonon region for As_2S_3, As_2Se_3, and mixed As_2S_3-As_2Se_3 and As_2Se_3-$GeSe_2$ glasses, and measurement of the temperature dependence of absorption coefficients in the multiphonon region for As_2Se_3 glass.

14. KEY WORDS	LINK A		LINK B		LINK C	
	ROLE	WT	ROLE	WT	ROLE	WT
Glass						
Infrared						
Chalcogenide						
CO_2 Laser						
Window						
Arsenic						
Selenium						
Multiphonon						

SUMMARY

A quantitative study of infrared absorption in the 250-4000 cm^{-1} region of As_2Se_3 glasses doped with small amounts of As_2O_3 or purified by various procedures has been carried out with particular attention to absorption in the wavelength regions of the CO_2 and CO lasers. The dependence of the relative intensities of the oxide impurity bands in the 650-1340 cm^{-1} region on the total amount of As_2O_3 added to the glass indicates the existence of three distinct oxide impurity species. A number of higher frequency impurity bands which are due to the presence of hydrogen in the glass and whose intensities are highly dependent on the glass melting conditions have been observed and classified. Absorption coefficients of As_2Se_3 glass in the 920-1090 cm^{-1} CO_2 laser region are limited by intrinsic multiphonon absorption to values of around 10^{-2} cm^{-1}. The lowest absorption coefficients measured in the 1700-2000 cm^{-1} CO laser region were around 2×10^{-3} cm^{-1} and may contain contributions from hydrogen impurity bands.

Intrinsic multiphonon absorption coefficients of mixed As_2Se_3-$GeSe_2$ glasses were found to be of the same magnitude at the same respective frequencies as those for pure As_2Se_3 glass. Hence selenide glasses are unsuitable as windows for high power CO_2 lasers.

SUMMARY p.2

The "molecular model" of Lucovsky and coworkers for vibrational properties of chalcogenide glasses such as As_2S_3, As_2Se_3, GeS_2 and $GeSe_2$ suggests that multiphonon absorption in these materials should be analogous to overtone and combination vibrational bands in isolated molecules. A variety of experiments have been carried out whose results are in reasonable accord with this prediction. These include Raman spectra of As_2S_3 glass, measurement of the frequency dependence of infrared absorption in the multiphonon region for As_2S_3, As_2Se_3, and mixed As_2S_3-As_2Se_3 and As_2Se_3-$GeSe_2$ glasses, and measurement of the temperature dependence of absorption coefficients in the multiphonon region for As_2Se_3 glass.

PUBLICATIONS RESULTING FROM RESEARCH SUPPORTED BY CONTRACT NO. N00014-67-A-0377-0017

1. "Infrared Transmission of As_2Se_3 Glass." C.T. Moynihan, P.B. Macedo, M. Maklad, and R. Mohr, in "Conference on High Power Infrared Laser Window Materials," Vol. II, C.A. Pitha, Ed., AFCRL-TR-73-0372 (II), 19 June 1973, Special Reports, No. 162 pp. 705-725.

2. "Infrared Transmission in Chalcogenide Glasses." M. Maklad, R. Mohr, R. Howard, P.B. Macedo and C.T. Moynihan, in "Third Conference on High Power Laser Window Materials," Vol.I, C.A. Pitha and B. Bendow, Eds., AFCRL-TR-74-0085 (I), 14 February 1974, Special Reports, No. 174, pp. 69-95.

3. "Multiphonon Absorption in As_2S_3-As_2Se_3 Glasses." M.S. Maklad, R.K. Mohr, R.E. Howard, P.B. Macedo, and C.T. Moynihan, Solid State Commun., 15, 855 (1974).

4. "Dependence of the Glass Transition Temperature on Heating and Cooling Rate." C.T. Moynihan, A.J. Easteal, J. Wilder, and J. Tucker, J. Phys. Chem. 78, 2673 (1974).

5. "Intrinsic and Impurity Infrared Absorption in As_2Se_3 Glass." C.T. Moynihan, P.B. Macedo, M.S. Maklad, R.K. Mohr. and R.E. Howard, J. Non-Cryst. Solids, in press.

6. "Multiphonon Absorption in Chalcogenide Glasses." R.E. Howard, P.S. Danielson, M.S. Maklad, R.K. Mohr, P.B. Macedo, and C.T. Moynihan, in "Optical Properties of Highly Transparent Solids," S.S. Mitra and B. Bendow, Eds., Plenum Press, in press.

Journal of Non-Crystalline Solids 17 (1975)

INTRINSIC AND IMPURITY INFRARED ABSORPTION IN As_2Se_3 GLASS

C.T. MOYNIHAN, P.B. MACEDO, M.S. MAKLAD,
R.K. MOHR and R.E. HOWARD
Vitreous State Laboratory, Departments of Chemical Engineering and Materials Science and Physics, The Catholic University of America, Washington, D.C. 20064, USA

Received 17 September 1974

A quantitative study of infrared absorption in the 250–4000 cm^{-1} region of As_2Se_3 glasses doped with small amounts of As_2O_3 or purified by various procedures has been carried out with particular attention to absorption in the wavelength regions of the CO_2 and CO lasers. The dependence of the relative intensities of the oxide impurity bands in the 650–1340 cm^{-1} region on the total amount of As_2O_3 added to the glass indicates the existence of three distinct oxide-impurity species. A number of higher-frequency impurity bands which are due to the presence of hydrogen in the glass and whose intensities are highly dependent on the glass-melting conditions have been observed and classified. Intrinsic multiphonon absorption in the 400–1100 cm^{-1} region has been interpreted in terms of combination and overtone bands of the two highest-frequency fundamental vibrational modes. Absorption coefficients of As_2Se_3 glass in the 920–1090 cm^{-1} CO_2 laser region are limited by intrinsic multiphonon absorption to values of around 10^{-2} cm^{-1}. The lowest absorption coefficients measured in the 1700–2000 cm^{-1} CO laser region were around 2×10^{-3} cm^{-1} and may contain contributions from hydrogen-impurity bands.

1. Introduction

Selenide glasses are an important class of infrared-transmitting materials [1]. Probably the most widely studied selenide glass is As_2Se_3, but the numerous studies of infrared absorption in this material [2–14] have provided very little in the way of quantitative assessment of absorption in wavelength regions of high transparency. On the other hand, the recent development and commercial availability of high-power infrared lasers have created a need for information about the inherent limits of absorption in infrared-transmitting materials [1, 15]. Consequently, we have carried out a quantitative study of impurity and bulk absorption in As_2Se_3 glass, with particular attention to absorption at the wavelengths of the CO_2 laser (9.2–10.8 μm, 1090–920 cm^{-1}) and of the CO laser (5–6 μm, 2000–1700 cm^{-1}).

The two principal sources of IR absorption in As_2Se_3 glasses are light atom impurities (oxygen and hydrogen) [1, 4–8, 11, 13] and intrinsic multiphonon pro-

cesses [1, 6, 13]. Hence, two lines of investigation were pursued by us. First, the magnitude of excess absorption of As_2Se_3 glasses doped with known amounts of oxide impurity was determined. Second, the absorption of As_2Se_3 glasses prepared using a variety of purification procedures was measured to fix unambiguously the intrinsic absorption coefficients.

2. Sample preparation and purification

As_2Se_3 glasses were compounded in batches of about 15 g from commercially available high-purity As (Cominco American, 99.9999%) and Se (Atomergic Chemicals Co., 99.9999%). These were stored, weighed, and handled in a Vacuum Atmospheres N_2-filled inert atmosphere box to avoid any contamination from atmospheric oxygen and moisture. Primary standard As_2O_3 was used as a dopant.

In the "standard" preparation procedure 1.3 cm od, 1.0 cm id Vycor melt tubes were sealed at one end, heated with a torch under vacuum to remove adsorbed water, and transferred to the inert atmosphere box. The glass components were loaded into the tubes, which were then removed from the box and sealed off under vacuum. The glasses were melted for 20 h at 850°C in a rocking furnace, removed from the furnace and cooled in air, annealed inside the melt tubes for a few hours at 155–170°C, cooled slowly to room temperature, and removed from the melt tubes.

Several special purification procedures designed to eliminate oxide impurities were also tried [1, 7]. These included:

(1) Baking the Vycor melt tubes overnight under vacuum at 850–900°C to remove adsorbed water before loading the glass components.

(2) Baking the components overnight at 100–120°C in the melt tubes under vacuum before sealing off to remove surface moisture from the components.

(3) Addition to the melt components of small amounts of metallic Al or Zr to act as oxide getters.

(4) Distillation of the glass. The glass after melting was sealed into one side of a 1.3 cm od Vycor tube divided into two sections by a coarse-porosity Vycor fritted disc. With the distillation tube in a horizontal position the glass was heated to 800–850°C so that it distilled through the fritted disc and into the second side which was held at a lower temperature. Ordinarily the distillation was carried out with the distillation tube sealed under vacuum, but distillations were also carried out with the tube sealed at room temperature under $\frac{1}{3}$ atm of N_2, H_2 or 5% H_2 – 95% N_2. Following distillation the glass was remelted briefly at 700–850°C in Vycor sealed under vacuum and then annealed. Vacuum distillations were intended to degas the glass and remove involatile impurities; distillations under H_2 were intended to lead to oxide removal by formation of H_2O. The fritted disc served to prevent carry-over of particulate matter during the distillation.

As_2Se_3 glasses quantitatively doped with small amounts of As_2O_3 were prepared

by dilution procedures. Several batches of As_2Se_3 glass to which had been added 910 ppm As_2O_3 were melted, where "ppm" refers to the content of added impurity on a molar basis. Glasses containing less than 910 ppm As_2O_3 were obtained both by remelting the 910 ppm glass with previously prepared undoped As_2Se_3 glass and by remelting the 910 ppm glass with appropriate amounts of elemental As and Se. Glasses of the same nominal As_2O_3 content prepared by the two different dilution procedures were within experimental error indistinguishable on the basis of their infrared absorption.

3. Infrared absorption measurements

Samples for IR absorption measurements were prepared by cutting slices from the 1.0 cm od glass boules and polishing the opposite faces plane parallel. Sample thicknesses ranged from 0.018 to 2.5 cm. The polished specimens were examined under an IR microscope, and those found to contain bubbles or gross amounts of particulate matter were not used for transmission measurements.

IR spectra over the range 250–4000 cm^{-1} (40–2.5 μm) were measured at ambient temperature with a Perkin–Elmer Model 467 double beam spectrometer with a variable attenuator in the reference beam. Prior to recording the spectrum the attenuator was set to give a reading of 100% transmission with no sample in the sample beam. A typical spectrum of an oxide-free As_2Se_3 glass is shown in fig. 1.

The absorption coefficient α was obtained from the transmission T, the sample thickness x, and the reflectivity R by the equation

$$T = (1-R)^2 \exp(-\alpha x)/[1 - R^2 \exp(-2\alpha x)] . \quad (1)$$

which is valid for normal incidence of the light beam on the sample surface in regions in which $\alpha\lambda \ll 1$, where λ is wavelength. The reflectivity R used in eq. (1) was calculated from the transmission T_0 measured on the same spectrum in regions of negligible absorption (the flat regions of the spectrum where $\alpha x \ll 1$, see fig. 1):

$$T_0 = (1-R)^2/(1-R^2) . \quad (2)$$

The average value of T_0 in the 7–10 μm region for 34 different As_2Se_3 samples in our study was 0.63 ± 0.01. This agrees well with the T_0 value of 0.64 calculated from published values [3, 5, 6] of the refractive index n using eq. (2) and the relation

$$R = (n-1)^2/(n+1)^2 .$$

Slight differences between the T_0 values obtained from the IR spectrum and from the index of refraction may arise because of slight deviations from normal light incidence or because of scattering from small surface imperfections or foreign-material inclusions in the sample in the IR spectrum determination.

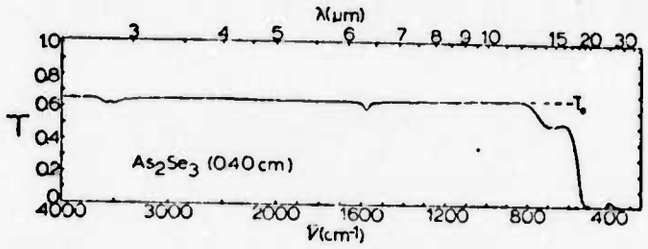

Fig. 1. Infrared spectrum of As_2Se_3 glass prepared by the "standard" procedure. Sample thickness 0.40 cm.

Calorimetric absorption coefficient measurements in the CO_2 and CO laser-wavelength regions were carried out at ambient temperature using Molectron Corp. model C250 tunable CO_2 and CO lasers and a CRL model 20 power meter. The method described by Pinnow and Rich [16] with the sample mounted outside the laser cavity was employed. Heat capacities needed for the calorimetric α calculation were taken from the paper of Schnaus et al. [17].

4. Oxide impurity absorption

In fig. 2 are shown IR spectra of thin samples of As_2O_3-doped As_2Se_3 glasses of comparable thickness. Jerger and Sherwood [5] and Vasko et al. [11] have observed that As_2Se_3 spectra in the region shown in fig. 2 depend only on the total amount

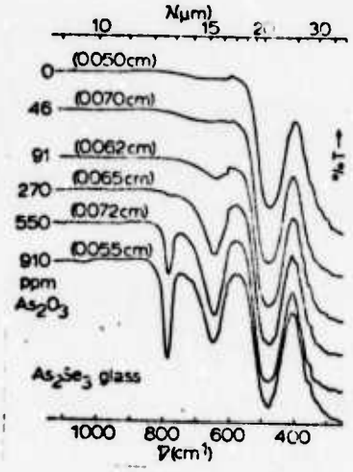

Fig. 2. Infrared spectra of thin samples of As_2O_3-doped As_2Se_3 glasses. Sample thicknesses shown in parentheses. The discontinuities in the spectra at 600 cm^{-1} are due to a grating change in the spectrometer.

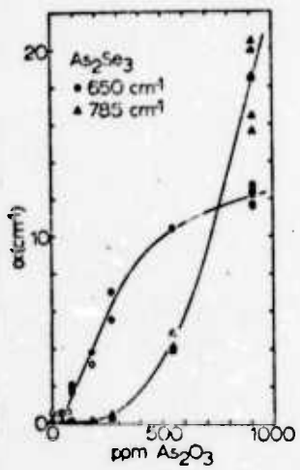

Fig. 3. Absorption coefficient versus ppm added As_2O_3 for As_2Se_3 glasses for the 650 and 785 cm^{-1} oxide impurity band maxima.

of oxygen present and are independent of whether the oxygen was added to the melt components in the form of As_2O_3 or SeO_2. The principal features of fig. 2 are (1) a strong peak at 480 cm^{-1} whose intensity is independent of oxide content and which hence must be an intrinsic absorption band, (2) an oxide impurity band at 650 cm^{-1} which becomes noticeable at 91 ppm As_2O_3 and grows rapidly with further additions of As_2O_3 up to 550 ppm and less rapidly thereafter, and (3) an oxide impurity band at 785 cm^{-1} which first appears at 270 ppm and grows rapidly with further As_2O_3 additions. Plots of the absorption coefficient at the 650 and 785 cm^{-1} oxide band maxima versus ppm of added As_2O_3 are shown in fig. 3.

The presence in As_2Se_3 glasses of two principal oxide absorption peaks at 650 cm^{-1} and 785 cm^{-1} whose relative intensities varied with the glass preparation was first noted by Vasko et al. [11]. On the basis of the spectra of the various forms of pure As_2O_3 they concluded that the 785 cm^{-1} band was due to oxygen present as As_4O_6 molecules (As_2O_3 form I), while the 650 cm^{-1} band was due to oxygen present in a network structure similar to that of vitreous As_2O_3 or of the As_2O_3 monoclinic crystal (As_2O_3 form II).

The solubility of As_2O_3 in As_2Se_3 glass is roughly 2000 ppm [18]. Hence in the glasses of fig. 2 the As_2O_3 is dissolved in the As_2Se_3 on a molecular level. Figs. 2 and 3 show that the oxide species associated with the 650 cm^{-1} band (form II) predominates at low concentrations, but as the total concentration of As_2O_3 increases, the concentration of the 650 cm^{-1} species begins to level off, and further As_2O_3 increments end up in the glass mainly in the form of the oxide species associated with the 785 cm^{-1} band (form I). These two pieces of evidence support the conclusions of Vasko et al. [11], so that we may tentatively relate the 650 cm^{-1} band to vibrations of oxygen incorporated substitutionally for selenium in the As_2Se_3

network in the form of ≥As–O–As≤ local groups, while the 785 cm^{-1} band may be associated with vibrations of As_4O_6 molecules dissolved in the glass. The relative concentrations of the two species would be controlled by an equilibrium of the form

$$4\,\text{As (network)} + 6\,\text{O (network)} \rightleftarrows \underset{\text{(form II, 650 cm}^{-1}\text{)}}{\text{As}_4\text{O}_6\ \text{(dissolved in melt)}} \qquad \underset{\text{(form I, 785 cm}^{-1}\text{)}}{} \qquad (3)$$

which would strongly favor form II at low overall oxygen concentrations and favor form I at high concentrations. In view of the very broad miscibility gap (0.2–98 mol% As_2O_3) in the As_2Se_3 – As_2O_3 system [18], which indicates a pronounced lack of affinity between the oxide and the selenide, the displacement of eq. (3) to the right with increasing overall oxide content and the concomitant aggregation of oxygen into As_4O_6 molecules may be viewed as a precursor step to the gross segregation of oxygen into a separate phase that takes place above 2000 ppm As_2O_3.

A point of some concern to us with regard to our doping experiments was that, since As_2O_3 is highly volatile, the As_2O_3 vapor pressure over the As_2Se_3 melt might be sufficiently high for a substantial portion of the added As_2O_3 to be segregated into the vapor phase above the melt at high temperatures and hence not to appear in the quenched glass. To check on this possibility we carried out a number of syntheses of 910 ppm As_2O_3 glasses in which we varied both the ratio of the volume of the empty space in the sealed melt tube to the melt volume, V_{void}/V_{melt}, and the melt temperature. The absorption coefficients at the 650 and 785 cm^{-1} oxide bands for these glasses are shown in table 1. The α values at 650 cm^{-1} are all identical within experimental error; however, the intensity of the 650 cm^{-1} band is not greatly sensitive to the total amount of oxide at concentrations around 910 ppm. The α values at 785 cm^{-1} show a scatter of about ± 10% about their mean. From fig. 3 one may estimate that about 400 ppm of As_2O_3 are in form I associated with the 785 cm^{-1} band, so that the scatter in the 785 cm^{-1} α values corresponds to an un-

Table 1
Absorption coefficients at 650 and 785 cm^{-1} of As_2Se_3 glasses doped with 910 ppm As_2O_3.

Melt history	V_{void}/V_{melt}	α_{650} (cm^{-1})	α_{785} (cm^{-1})
20 h at 850°C	–	12.4	20.4
20 h at 850°C	1.8	12.7	19.9
20 h at 850°C	3.7	11.7	18.6
20 h at 850°C	5.5	11.6	15.6
2 h at 550°C, 20 h at 850°C	–	12.3	16.4
20 h at 850°C, 20 h at 450°C	–	12.2	16.4
20 h at 450°C	2.9	12.3	18.4
Average		12.2 ± 0.3	18.0 ± 1.6

certainty of about ± 40 ppm in the total 910 ppm As_2O_3 content or about ± 0.3 mg As_2O_3 in a 15 g batch. This is very close to the estimated accuracy of our As_2O_3 addition procedure, so that the scatter may be primarily due to experimental uncertainty from this source. Alternatively, the scatter in the 785 cm^{-1} values may be due to the extraction of varying amounts of oxide (of the order of 50 ppm) by the Vycor melt container, as explained in sect. 5. The absence of changes in the 785 cm^{-1} α value with changes in melt temperature large enough to produce large differences in the As_2O_3 vapor pressure, however, demonstrates fairly conclusively that a negligible amount of oxide is lost as vapor into the void space above the melt.

The temperature independence of the 650 and 785 cm^{-1} α values of table 1 also indicates that at 910 ppm As_2O_3 the relative amounts of the two forms of As_2O_3 impurity in the glass are independent of melt temperature. This may mean that the reaction of eq. (3) is extremely rapid at 450°C and above, so that the relative amounts of the two species observed in the glass correspond to the equilibrium concentrations at some temperature below 450°C at which the rate of eq. (3) becomes sufficiently slow that the reaction is arrested during the cooling of the glass. Alternatively, if one assumed that the rate of eq. (3) was sluggish compared to the cooling rate at all temperatures at and below 850°C, then the results of table 1 would indicate that the equilibrium constant for eq. (3) and hence the relative amounts of the two oxide species have very little temperature dependence. This is not an unreasonable presumption, since in eq. (3) there is no net breakage of As–O bonds, one As–O bond being formed in a As_4O_6 molecule for every As–O bond broken in the network. Hence, the enthalpy change and consequently the temperature dependence of the equilibrium constant for eq. (3) may be quite small.

It is of interest to note that the existence of two different oxide species in vitre-

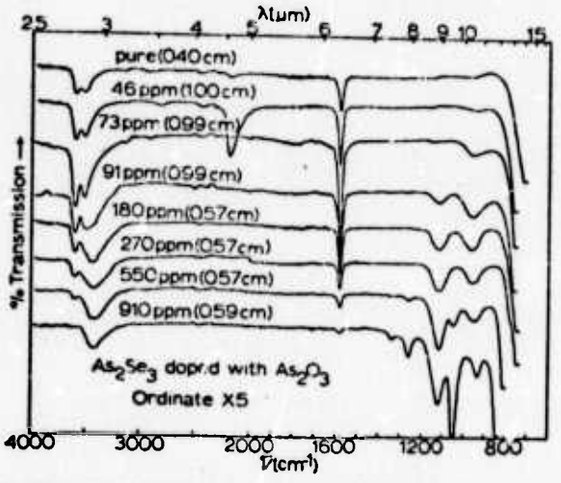

Fig. 4. Expanded ordinate (× 5) infrared spectra of thick samples of As_2O_3-doped As_2Se_3 glasses. Sample thickness shown in parentheses.

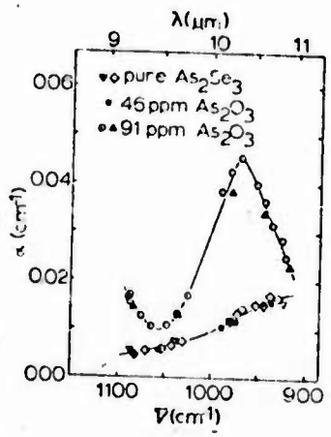

Fig. 5. Calorimetric absorption coefficients versus wavenumber for As_2Se_3 glasses measured with the CO_2 laser.

ous selenium has also been detected by infrared spectroscopy [19, 20].

Oxide impurities in As_2Se_3 also give rise to a number of weaker absorption bands in the 900–1400 cm^{-1} region, some of which have been noted previously [5–7, 11]. These are shown in the expanded ordinate spectra of thick As_2O_3-doped As_2Se_3 glasses in fig. 4. The growth of the weak band at 1125 cm^{-1} with increasing As_2O_3 content correlates with the growth of the 650 cm^{-1} band of fig. 2, so that both these bands may be assigned to impurity oxygen incorporated into the As_2Se_3 network (form II). Similarly the growth of the weak bands at 1050, 1265, and 1340 cm^{-1} correlate with the growth of the 785 cm^{-1} band in fig. 2, so that all these bands may be assigned to As_4O_6 molecules dissolved in the melt (form I). The growth of the weak 965 cm^{-1} band in fig. 4 correlates with the growth of neither the 650 nor the 785 cm^{-1} bands in fig. 2, so that this band must correspond to yet a third impurity oxide species (form III) whose concentration is presumably small compared to that of form II. This 965 cm^{-1} band appears to grow in strength with increasing As_2O_3 content up to about 300 ppm and to saturate thereafter. As the moment we cannot unambiguously identify the origin of this 965 cm^{-1} band. Although Vasko et al. [11] have demonstrated fairly clearly that impurity oxygen in As_2Se_3 bonds preferentially to As, it is possible that a small but detectable fraction of the oxygen bonds to Se and that the 965 cm^{-1} band may be due to Se–O vibrations. One of the oxide impurity species in vitreous selenium has a IR band at 925 cm^{-1} [19, 20], not far removed from the observed frequency of 965 cm^{-1} of form III in As_2Se_3. It is this 965 cm^{-1} band which is primarily responsible for oxide impurity absorption in As_2Se_3 in the wavelength region of the CO_2 laser, as shown in calorimetric absorption coefficient data of fig. 5.

The various oxide impurity bands are classified in table 2.

Table 2
Bulk and impurity absorption maxima in As_2Se_3 glass in the 2.5–40 μm region.

ν (cm^{-1})	λ (μm)	Relative intensity [a]	Assignment
< 250	> 40	vs	fundamental $AsSe_3$ stretch
340	29	s	shoulder, fundamental As–Se–As stretch (?)
480	20.8	s	intrinsic 2-phonon process
690	14.5	m	intrinsic 2- and 3-phonon processes
880	11.4	w	shoulder, intrinsic 3- and 4-phonon processes
785	12.7	s	oxide form I, molecular As_4O_6
1050	9.5	w	
1265	7.9	vw	
1340	7.5	vw	
650	15.4	s	oxide form II, network >As–O–As<
1125	8.9	w	
965	10.4	w	oxide form III, –Se–O– (?)
1585	6.3	w	H_2O dissolved in glass
3520	2.84	w	
3600	2.78	w	
3420	2.92	w	–O–H in glass containing As_2O_3
630	15.9	vw	H_2Se, –Se–H and related structural features
1280	7.8	vw	
2190	4.57	w	
2430	4.12	vw	
2830	3.53	vw	

[a] vs = very strong, s = strong, m = medium, w = weak, vw = very weak.

5. Oxide extraction by the melt container

Dissolution of the silica-glass melt container has been suggested as a possible source of oxide contamination of chalcogenide glasses [7, 8]. To determine whether this was a source of oxide contamination in our As_2Se_3 glasses, rather early in our study we carried out a series of syntheses using starting materials from the same batch in which we varied both the melting time and the melting temperature. Our initial thought was that oxide contamination from melt-container dissolution should increase with increases in melting time and melting temperature. Infrared spectra of these glasses are shown in fig. 6. We found, surprisingly, that the intensity of the 650 cm^{-1} oxide band decreased with increases in melting time and melting temper-

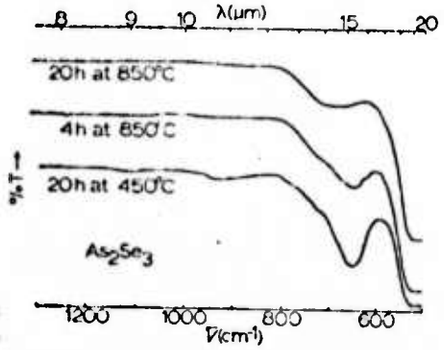

Fig. 6. Infrared spectra of As_2Se_3 glasses melted in Vycor as a function of melting time and melting temperature. Sample thicknesses 0.40 cm.

ature. Evidently the starting materials for the glasses of fig. 6 were contaminated with oxide, and this oxide was removed by an extended, high-temperature melt in Vycor.

Further evidence for removal of small amounts of oxide during melting of As_2Se_3 is seen in figs. 2 and 3 in which the absorption coefficient at the 650 cm^{-1} oxide maximum does not depart from the value for the undoped glass until over 50 ppm As_2O_3 have been added. Similarly figs. 4 and 5 show that the absorption coefficients near the 965 cm^{-1} oxide maximum are the same for undoped As_2Se_3 and As_2Se_3 to which 46 ppm of As_2O_3 have been added.

The only two reasonable explanations for the disappearance of small amounts of oxide during melting are (1) segregation of the oxide into the vapor phase above the melt, and (2) extraction of the oxide by diffusion into the walls of the silica-melt container. The first explanation may be ruled out on the basis of the evidence presented in table 1 and the discussion in sect. 4. In addition, the vapor pressure and concentration of oxide above the melt should depend on the oxide concentration in the melt via a form of Henry's law appropriate to eq. (3). This in turn would require that the α-versus-ppm As_2O_3 plot at 650 cm^{-1} of fig. 3 show a continuous, monotonic fall with decreasing ppm As_2O_3 all the way down to zero ppm As_2O_3, rather than the abrupt break at around 50 ppm As_2O_3 that it does in fact display.

The second explanation, diffusion of the As_2O_3 into the walls of the Vycor melt container, is not unreasonable in view of, on the one hand, the lack of affinity between As_2Se_3 and As_2O_3 demonstrated by the large immiscibility gap in this system, and on the other hand, the affinity of As_2O_3 for a silicate network demonstrated by the fact that As_2O_3 can be included in numerous homogenous oxide glasses. The amount of oxide removed by this process is probably kinetically controlled by the slow rate of diffusion of the As_2O_3 into the Vycor glass network and should increase with increases in melting temperature, melting time, and Vycor glass area in the interior of the melting tube. On this basis, one would expect that an oxide melt should

be considerably more effective than the Vycor glass in extracting oxide impurities from an As_2Se_3 melt. To test this supposition, we remelted 15.5 g of previously prepared As_2Se_3 glass containing 910 ppm of added As_2O_3 with 5.0 g of B_2O_3 for 20 h at 850°C. The B_2O_3 is quite fluid at this temperature and is extremely immiscible with the As_2Se_3 melt, as shown by the fact that no new oxide bands due to B–O vibrations were observed in the extracted As_2Se_3. The absorption coefficients of the glass extracted with B_2O_3 were 5.6 cm^{-1} at 650 cm^{-1} and 0.31 cm^{-1} at 785 cm^{-1} compared with 12.2 cm^{-1} at 650 cm^{-1} and 18.0 cm^{-1} at 785 cm^{-1} (table 1) for the unextracted 910 ppm glass. From fig. 3 these α values are seen to correspond to a concentration of about 240 ppm As_2O_3 in the extracted glass, so that the B_2O_3 extraction removed about 75% of the As_2O_3 initially present in the As_2Se_3.

For the melt times and temperatures and melt tube sizes used in most of our oxide doping experiments the amount of As_2O_3 extracted by the Vycor glass melt tube seems to be no more than about 50 ppm. Consequently, the actual As_2O_3 contents of our doped glasses are likely to be some 50 ppm lower than the ppm of added As_2O_3 indicated in figs. 2–5.

6. Hydrogen impurity absorption

As shown in figs. 1, 4 and 7, a variety of high-frequency IR absorption bands appear in As_2Se_3. These bands have previously been attributed to hydrogen impurities [4, 6, 7], and their occurrence and intensity depend strongly on preparation

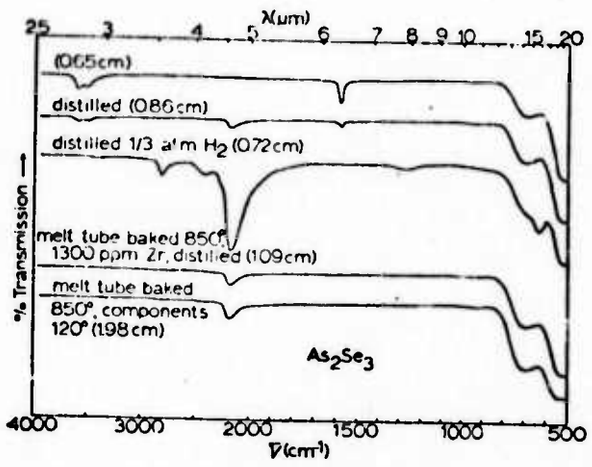

Fig. 7. Infrared spectra of As_2Se_3 glasses prepared using various special purification procedures. The glass of the topmost spectrum was prepared by the "standard" procedure. Sample thicknesses shown in parentheses.

conditions. As_2Se_3 glasses prepared by the "standard" procedure (fig. 1 and topmost spectrum of fig. 7) exhibit a set of bands at 1585, 3520 and 3600 cm^{-1} which are always of the same relative intensity with respect to one another, but whose absolute intensities vary from batch to batch. These same bands are observed in a wide variety of other selenide and sulfide glasses [4, 6, 21] and are usually attributed to O–H vibrations. It seems likely that they are due to molecular H_2O dissolved in the glass rather than O–H groups bonded in turn to the network, e.g. >As–O–H, since their presence does not give rise to any excess absorption in the wavelength region in which As–O vibrations manifest themselves, as detailed below. Indeed, allowing for a slight shift to lower frequencies due to hydrogen bonding to the network, the frequencies of these bands agree rather nicely with the fundamental vibrational frequencies of isolated H_2O molecules (1595, 3657 and 3756 cm^{-1}). The H_2O must be adsorbed initially on the silica melt tube or on the components, since the bands do not occur when the melt tube and components are baked before melting the glass, as shown by the bottom spectrum of fig. 7.

When substantial amounts of As_2O_3 are added to the As_2Se_3 glass, these H_2O bands gradually shift in character, as shown in fig. 4. The 1585 cm^{-1} band becomes greatly reduced in relative intensity, while the 3520 and 3600 cm^{-1} bands are replaced by one at 3420 cm^{-1}. This merging of the two molecular water stretching vibrations (3520 and 3600 cm^{-1}) into a single vibration at 3420 cm^{-1} and the disappearance of the 1585 cm^{-1} H_2O bending vibration suggest that in the presence of excess oxide the molecular H_2O vanishes via a reaction of the form

$$>As–O–As< + H_2O \rightarrow 2\ >As–O–H .$$

The As–O–H groups should exhibit a single O–H stretching frequency close to the O–H group frequency typically observed in organic compounds (3500–3700 cm^{-1}).

As shown in fig. 7, in undoped As_2Se_3 glasses which have been melted after baking of the melt tube and components or to which have been added reducing agents such as Zr or Al the H_2O bands are replaced by a band at 2190 cm^{-1}. Distillation of the melt under H_2 enhances this band considerably, as has been observed previously [6, 7], and reveals a number of associated weaker bands at 630, 1280 2430 and 2830 cm^{-1}. The 1280, 2190, 2430 and 2830 bands are probably associated with impurity H_2Se or –Se–H vibrations [6, 7]. (For comparison, the isolated H_2Se fundamental frequencies are 1034, 2345 and 2358 cm^{-1}.) The 630 cm^{-1} band, which is at a rather low frequency for a light-atom vibration, is likely due to bulk As or Se atom vibrations in a local structural group produced by the hydrogen, e.g., a >As–Se–H group.

In some As_2Se_3 glasses hydrogen-impurity bands due to both H_2O and H_2Se vibrations can be observed, e.g., the second spectrum from the top in fig. 7. Thus far we have not succeeded in producing an As_2Se_3 glass in which all of the hydrogen-impurity bands have been reduced to an indectable level. These bands are listed and classified in table 2.

Table 3
Calorimetric absorption coefficients of As_2Se_3 glasses measured with CO laser.

Special purification procedures	ν (cm^{-1})	λ (μm)	α (cm^{-1}
Distilled under 5% H_2–95% N_2	1900 a)	5.25 a)	0.021
Distilled under vacuum	1900 a)	5.25 a)	0.0084
None	1900 a)	5.25 a)	0.007
91 ppm As_2O_3 added	1900 a)	5.25 a)	0.0056
910 ppm As_2O_3 added	1980	5.05	0.0040
	1920	5.20	0.0024
	1890	5.28	0.0026

a) Untuned laser.

7. Absorption in the CO laser region

Calorimetric absorption coefficients of As_2Se_3 glasses measured with the CO laser are listed in table 3. For the measurement on the 910 ppm As_2O_3 glass the laser was tuned to specific wavelengths. For the other glasses the measurement was carried out with the untuned laser for which the "center of gravity" of the multiline output intensity-versus-wavelength plot lies at 5.25 μm (1900 cm^{-1}). The glasses are arranged in order of decreasing intensity of the 4.57 μm (2190 cm^{-1}) H_2Se

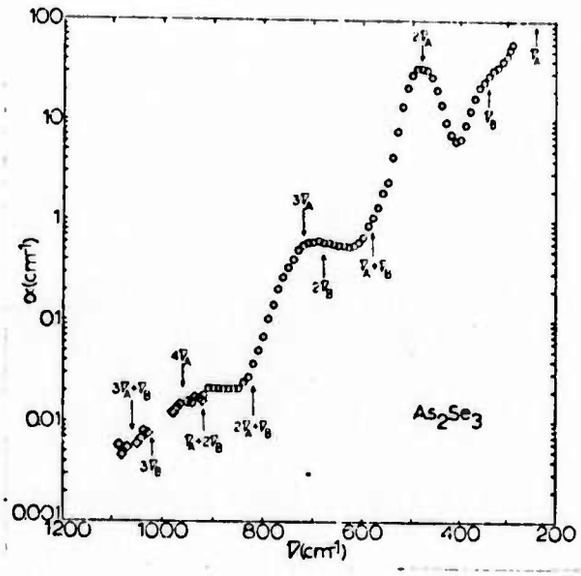

Fig. 8. Absorption coefficient versus wavenumber for pure As_2Se_3 glass in the multiphonon absorption region. $\bar{\nu}_A$ = 240 cm^{-1}, $\bar{\nu}_B$ = 340 cm^{-1}. ◇ calorimetric α values, ○ IR spectra α values.

impurity band as observed on the IR spectra (see figs. 4 and 7). The α values of table 3 decrease in the same order, and it seems clear that the higher values of α observed at the CO laser wavelengths are due to the low-frequency tail of this 4.57 μm H_2Se impurity band. Somewhat ironically, the oxide-doped glasses which are the worst transmitters at CO_2 laser wavelengths are the best transmitters in the CO laser wavelength region. Even with the 910-ppm As_2O_3 glass the absorption coefficient is still decreasing as one moves away from the 4.57 μm H_2Se band position, so that the lowest α values of around 2×10^{-3} cm^{-1} observed in this experiment can still be considered only an upper limit to the intrinsic absorption of As_2Se_3 glass in the 5–6 μm region.

8. Intrinsic absorption below 1100 cm^{-1}

In table 4 are listed absorption coefficients at the 650 cm^{-1} impurity oxide absorption frequency and at 943 cm^{-1} (10.6 μm, the "nominal" operating wavelength of the CO_2 laser) for As_2Se_3 glasses prepared and purified by a variety of techniques. The good agreement among the α_{650} and the α_{943} values for the various samples suggests that these α values are intrinsic, that the glasses are all essentially free of oxide contaminant, and that the simple "standard" preparation is sufficient to prepare As_2Se_3 glasses with no impurity absorption in the frequency region 1100 cm^{-1} and below (9 μm and above).

Table 4
As_2Se_3 glass absorption coefficients at 650 cm^{-1} and 943 cm^{-1} (= 10.6 μm). All glasses melted 20 h at 850°C in Vycor sealed under vacuum. Duplicate α values at 650 cm^{-1} are for different samples from the same batch. Duplicate α values at 943 cm^{-1} were obtained on the same sample by different experimenters.

Special purification procedures	α_{650} (cm^{-1})	α_{943} (cm^{-1})
None	0.58	0.015
None	0.56	–
Distilled	0.53, 0.54	–
Distilled under N_2	0.63	0.016
Distilled under 5% H_2–95% N_2	0.57, 0.62	0.019
Melt tube baked at 850°C, components baked at 120°C	0.50, 0.52	–
Melt tube baked at 900°C, components baked at 100°C	0.53, 0.56	–
Melt tube baked at 850°C, 1300 ppm Al added, distilled	0.56	–
Melt tube baked at 850°C, 1300 ppm Zr added, distilled	0.51, 0.57	0.014, 0.015
46 ppm As_2O_3 added	0.61	0.012, 0.015
Average	0.56 ± 0.03	0.015 ± 0.001

In fig. 8 is shown a plot of intrinsic absorption coefficient-versus-wavenumber for As_2Se_3 glass in the 300–1100 cm^{-1} region. The principal features of fig. 8 and of the pure As_2Se_3 spectra of figs. 1, 2, 5, 6, and 7 are a shoulder at 340 cm^{-1}, maxima at 480 and 690 cm^{-1}, and a shoulder at 880 cm^{-1}. Previous investigators have noted the first three of these features [3–7, 11, 12].

Vitreous As_2Se_3 has an open-layered structure consisting of pyramidal $AsSe_3$ groups bridged by Se atoms (As–Se–As groups) [14, 22–25]. Lucovsky and Martin [14, 23] have suggested that in As_2Se_3 glass the $AsSe_3$ pyramidal groups are only weakly coupled vibrationally by the bridging As–Se–As groups and that the IR and Raman spectra in the fundamental region correspond to those for $AsSe_3$ molecules superimposed on much less intense As–Se–As spectra. The α values at the lowest frequencies in fig. 8 are due to the high-frequency tail of a fundamental band observed in IR, Raman, and reflectivity spectra at about 230 cm^{-1} [2, 3, 9, 10, 12–14, 26]; this is the most intense fundamental band in As_2Se_3 and has been assigned to $AsSe_3$ group stretching vibrations [14, 23]. The shoulder at 340 cm^{-1} in fig. 8 is probably also a fundamental, due possibly to an As–Se–As group stretching vibration [23, 27].

Above 400 cm^{-1} absorption coefficients of fig. 8 are due to multiphonon processes in which a high-energy photon couples weakly with a transverse optical mode of the solid, which TO mode then decays into two or more lower-energy phonons of frequencies corresponding to some fundamental vibrational mode. In terms of the molecular model of Lucovsky and Martin [14, 23] for the vibrational properties of As_2Se_3, multiphonon bands in this material become analogous to overtone or combination bands of isolated molecules. For a high-energy photon of a given frequency the most probable multiphonon process involves production of the minimum number of final-state phonons [28]. Consequently, in a material such as amorphous As_2Se_3 in which the density-of-vibrational-states-versus-frequency plot is highly structured, one expects similarly a highly structured $\alpha-\bar{\nu}$ plot in the multiphonon region which mirrors the density-of-states plot at the high-frequency end.

In fig. 8 we have indicated the frequencies corresponding to the overtones and combinations of two fundamental frequencies, $\bar{\nu}_A = 240$ cm^{-1}, which is close in frequency to the intense $AsSe_3$ stretching mode observed at about 230 cm^{-1}, and $\bar{\nu}_B = 340$ cm^{-1}, the frequency of the long-wavelength shoulder, possibly due to an As–Se–As stretch. The first few of these overtone and combination frequencies correspond clearly to prominent features in fig. 8, e.g., the maximum at 480 cm^{-1}, the change in slope at about 580 cm^{-1}, and the maximum at 690 cm^{-1}.

9. Conclusions

In the wavelength region of the CO_2 laser As_2Se_3 glass absorption coefficients appear to be limited by intrinsic multiphonon processes to values of the order of 10^{-2} cm^{-1}. Other selenide glasses, e.g., in the Ge–As–Se and Ge–Sb–Se systems,

are similar to As_2Se_3 in their nearest-neighbor reduced masses and bond-force constants, and hence a corresponding similarity in the multiphonon absorption coefficients in the CO_2 laser region is to be expected. Selenide glasses are thus markedly inferior in IR transparency in the CO_2 laser region to materials such as some alkali halides and semiconductor materials for which 10.6 μm absorption coefficients approaching 10^{-4} cm^{-1} have been measured [29].

As_2Se_3 intrinsic absorption coefficients in the CO laser region are no higher than 2×10^{-3} cm^{-1}.

Acknowledgements

The authors wish to thank P. Pureza, A. Marshall, C.Y. Kim, L. Marcondes, and M. Samanta for assistence with various aspects of the experimental program. This research was supported by the Advanced Research Projects Agency and monitored by the Office of Naval Research.

References

[1] A.R. Hilton, J. Non-Crystalline Solids 2 (1970) 28; J. Electronic Mater. 2 (1973) 211.
[2] J.T. Edmond, A. Anderson and H.A. Gebbie, Proc. Phys. Soc. 81 (1963) 378.
[3] J.T. Edmond and M.W. Redfearn, Proc. Phys. Soc. 81 (1963) 380.
[4] J.A. Savage and S. Nielsen, Phys. Chem. Glasses 5 (1964) 82.
[5] J. Jerger and R. Sherwood, Servo Corp. of America, Final Tech. Rept. Contract No. NONR-4212 (00) (1964).
[6] J.A. Savage and S. Nielsen, Infrared Phys. 5 (1965) 195.
[7] J.A. Savage and S. Nielsen, Phys. Chem. Glasses 6 (1965) 90.
[8] A.R. Hilton, C.E. Jones, R.D. Dobrott, H.M. Klein, A.M. Bryant and T.D. George, Phys. Chem. Glasses 7 (1966) 112, 116.
[9] E.J. Felty, G. Lucovsky and M.B. Myers, Solid State Commun. 5 (1967) 555.
[10] G. Lucovsky, Mat. Res. Bull. 4 (1969) 505.
[11] A. Vaško, D. Ležal and I. Sto, J. Non-Crystalline Solids 4 (1970) 311.
[12] P.C. Taylor, S.G. Bishop and D.L. Mitchell, Solid State Commun. 8 (1970) 1783.
[13] M. Onomichi, T. Arai and K. Kudo, J. Non-Crystalline Solids 6 (1971) 362.
[14] G. Lucovsky, Phys. Rev. B6 (1972) 1480.
[15] M. Sparks, J. Appl. Phys. 42 (1971) 5029.
[16] D.A. Pinnow and T.C. Rich, Appl. Opt. 12 (1973) 984.
[17] U.E. Selmaus, C.T. Moynihan, R.W. Gammon and P.B. Macedo, Phys. Chem. Glasses 11 (1970) 213.
[18] J.S. Berkes, paper presented at Amer. Ceramic Soc. Meeting, Glass Div., Chicago, Ill., April 26, 1971.
[19] R.A. Burley, Phys. Stat. Sol. 29 (1968) 551.
[20] J.D. Mackenzie, J. Non-Crystalline Solids 2 (1970) 16.
[21] P.A. Young, J. Phys. C 4 (1971) 93.
[22] R. Zallen, M.L. Slade and A.T. Ward, Phys. Rev. B3 (1971) 4257.
[23] G. Lucovsky and R.M. Martin, J. Non-Crystalline Solids 8–10 (1972) 185.

[24] D.D. Thornburg, J. Electronic Mater. 2 (1973) 495.
[25] A.J. Leadbetter and A.J. Apling, J. Non-Crystalline Solids 15 (1974) 250.
[26] J. Schottmiller, M. Tabak, G. Lucovsky and A. Ward, J. Non-Crystalline Solids 4 (1970) 80.
[27] M.S. Maklad, R.K. Mohr, R.E. Howard, P.B. Macedo and C.T. Moynihan, Solid State Commun. 15 (1974) 855.
[28] D.W. Pohl and P.F. Meir, Phys. Rev. Letters 32 (1974) 38.
[29] T.F. Deutsch, J. Phys. Chem. Solids 34 (1974) 2091.

MULTIPHONON ABSORPTION IN CHALCOGENIDE GLASSES

R.E. Howard, P.S. Danielson, M.S. Maklad, R.K. Mohr, P.B. Macedo and C.T. Moynihan

Vitreous State Laboratory, Catholic University of America, Washington, DC 20064

ABSTRACT

The "molecular model" of Lucovsky and coworkers for vibrational properties of chalcogenide glasses such as As_2S_3, As_2Se_3, GeS_2 and $GeSe_2$ suggests that multiphonon absorption in these materials should be analogous to overtone and combination vibrational bands in isolated molecules. A variety of experiments have been carried out whose results are in reasonable accord with this prediction. These include Raman spectra of As_2S_3 glass, measurement of the frequency dependence of infrared absorption in the multiphonon region for As_2S_3, As_2Se_3, and mixed As_2S_3-As_2Se_3 and As_2Se_3-$GeSe_2$ glasses, and measurement of the temperature dependence of absorption coefficients in the multiphonon region for As_2Se_3 glass.

INTRODUCTION

Chalcogenide glasses such as As_2S_3, As_2Se_3, GeS_2, and $GeSe_2$ possess open network structures of the types shown in Fig. 1. For example, As_2Y_3 glass (Y = S or Se) consists of pyramidal AsY_3 groups bridged by bent As-Y-As groups, while GeY_2 glass consists of tetrahedral GeY_4 groups bridged by bent Ge-Y-Ge groups. Lucovsky and his coworkers[1-4] have proposed a "molecular model" for the vibrational properties of glasses of this sort whose central feature is the pre-

sumption that the high coordination centers, e.g., the AsY_3 pyramidal groups or the GeY_4 tetrahedra, are coupled vibrationally to one another only very loosely by the bridging chalcogenide atoms. As a consequence their infrared and Raman spectra are to a first approximation expected to correspond to those of isolated AsY_3 or GeY_4 molecules superimposed on less intense spectra due to the bridging As-Y-As or Ge-Y-Ge groups. Raman and infrared spectroscopy studies of chalcogenide glasses in the fundamental region are in reasonable accord with the predictions of this model[1-6].

In solids multiphonon absorption takes place when a high energy photon couples weakly with a transverse optical mode of the material; this TO mode then decays into two or more lower energy phonons of frequencies corresponding to fundamental vibrational modes. For a high energy photon of a given frequency the most probable multiphonon absorption process involves production of the minimum number of final state phonons (see papers of Pohl and coworkers[7,8] and references cited therein). For crystalline materials such as the alkali halides the one phonon density of vibrational states is sizeable over a broad range of frequencies. This may be shown[7-9] to lead to a predicted absorption spectrum in the multiphonon region which is comparatively featureless at ambient temperature and above, in agreement with experiment.[9,10] For materials such as the chalcogenide glasses, however, the one phonon density of states is predicted by the molecular model to consist of a collection of discrete vibrational modes broadened only slightly by the small variations in local structure inherent to the amorphous state. Multiphonon absorption in these materials should then be restricted to relatively discrete frequencies $\bar{\nu}$ which satisfy the condition

$$\bar{\nu} = \sum_{i=1}^{n} \bar{\nu}_i \qquad (1)$$

where $\bar{\nu}_i$ are frequencies of the n fundamental modes into which the photon decays[11]. To put it another way, the molecular model predicts that multiphonon absorption processes in chalcogenide glasses should be analogous to combination and overtone bands in isolated molecules.

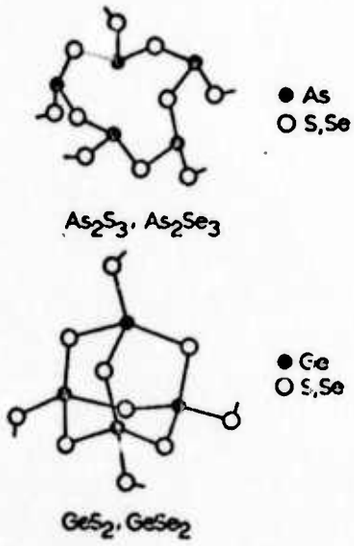

Figure 1. Local structure in chalcogenide glasses.

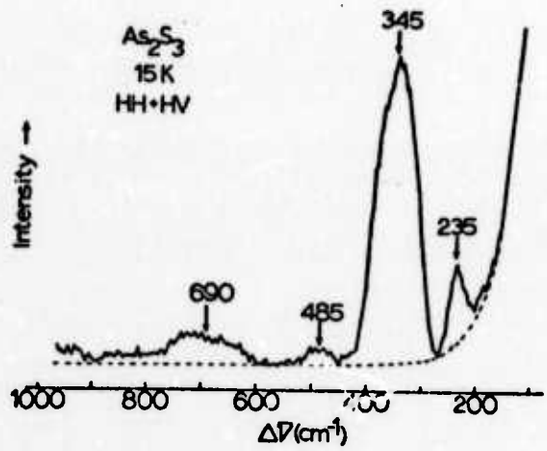

Figure 2. Raman spectrum of As_2S_3 glass at 15 K.

Further, because the probability of a given multiphonon process at a given frequency falls off rapidly with increasing number of final state phonons, n, multiphonon absorption in chalcogenide glasses should be dominated by combinations and overtones of the highest frequency fundamentals.

In the present paper we report the results of a number of experiments designed to test this hypothesis for multiphonon absorption in chalcogenide glasses. These include Raman spectroscopy of As_2S_3 glass, measurements of the frequency dependence of infrared absorption in the multiphonon region for As_2S_3, As_2Se_3, and mixed As_2S_3 - As_2Se_3 and As_2Se_3 - $GeSe_2$ glasses, and measurement of the temperature dependence of absorption coefficients in the multiphonon region for As_2Se_3 glass.

EXPERIMENTAL SECTION

Chalcogenide glasses were synthesized by reacting the elements (99.9999% purity) in evacuated Vycor tubes. Other preparation details are reported elsewhere[11,12]. Glass densities were determined from the masses and dimensions of the cylindrical specimens used for IR absorption measurements.

At most frequencies infrared absorption coefficients α were obtained from IR spectra of the glasses determined with a Perkin-Elmer Model 467 spectrometer[12]. IR spectra above ambient temperature were measured with the samples thermostatted in a small aluminum heating block; corrections to a spectrum for black-body emission from the hot sample were made using a blank spectrum run at the same temperature with the light beam to the sample blocked.

Absorption coefficient measurements for As_2Se_3 glass in the CO_2 laser wavelength region (920-1090 cm^{-1}) were carried out calorimetrically with a Molectron Corp. Model C250 tunable CO_2 laser and a CRL Model 201 power meter using previously described techniques[13,14]. For measurements above ambient temperature the sample was held in position at the ends of three Teflon-tipped screws and thermostatted in a cylindrical brass oven with baffles to eliminate spurious air currents and

24

and scattered radiation.

Raman scattering experiments on As_2S_3 glass were carried out using a Coherent Radiation Model 52 Ar ion laser (wavelength 514.5 nm), a Spex 1401 double monochromator (slit width 20 cm^{-1}), and an ITT FW130 photomultiplier as detector for the photon counting equipment. A 514.5 nm spike filter was placed between the laser beam and the sample to screen out any additional emission lines from the laser. The laser power was about 70 mw focused on a 0.5 mm diameter spot on the sample. To prevent excessive heating by the laser beam the sample was fashioned into a thin plate (0.16 mm thickness) and attached to an aluminum plate on the end of a cold finger with thermal paste and bonding resin. The angle between the incident laser beam and the normal to the sample surface was set equal to Brewster's angle (81.5° for As_2S_3); the scattered laser light was observed in a direction normal to the sample surface.

RAMAN SCATTERING FROM As_2S_3 GLASS

In Fig. 2 is shown the Stokes Raman spectrum of As_2S_3 glass at 15 K. The incident laser light was polarized in the scattering plane; the scattered laser light was unanalyzed. The laser wavelength (514.5nm) lies well inside the electronic absorption region of As_2S_3 glass, so that the intensity of scattered light has been increased considerably by resonance enhancement relative to the scattering intensity expected for incident laser light of wave length well outside the electronic absorption edge[15].

The spectrum of Fig. 2 is similar to those reported previously for As_2S_3 glass below 500 cm^{-1} [5,15,16]. The most pronounced feature is the large peak at 345 cm^{-1}, which has been attributed to stretching vibrations of AsS_3 pyramidal groups [1,2,5]. It presumably contains contributions from both the symmetric (344 cm^{-1}) and antisymmetric (310 cm^{-1}) stretching modes predicted by Lucovsky's molecular model treatment [1,2,5]. The 235 cm^{-1} peak of Fig. 2 is more intense than that in Ward's [16] or Kobliska and Solin's [5,15] spectra; its assignment is uncertain, but it may be due to a stretching vibration of a bent As-S-As group[1,5]. The small peak at 485 cm^{-1} has

also been observed by Kobliska and Solin[5,15] and by Ward[16]; its assignment is likewise somewhat uncertain, but it may also be due to a stretch of the bent As-S-As groups[1,3,5]. A S-S stretching vibration at 475 cm^{-1} is observed in the Raman spectra of Ward 16 for S-rich As-S glasses, but this appears to be distinct from the 485cm^{-1} As_2S_3 band. A similar weak 485 cm^{-1} band was also observed in GeS_2 glasses by Lucovsky et al., who likewise concluded that it was not due to S-S stretching vibrations[3].

The final prominent feature of Fig. 2, the weak band centered at 690 cm^{-1}, lies at a much higher frequency than any predicted fundamental modes of As_2S_3 glass[1,2,5]. Since it occurs at just twice the frequency of the strong 345 cm^{-1} band, it is reasonable to assign it via Eq. (1) to a 2-phonon scattering process, i.e., to the first harmonic of the AsS_3 pyramidal group stretching frequencies.

MULTIPHONON IR ABSORPTION IN As_2S_3 AND As_2Se_3 GLASSES

In Fig. 3 is shown a plot of IR absorption coefficient α versus wavenumber $\bar{\nu}$ for As_2S_3 and As_2Se_3 glasses in the multiphonon region at ambient temperature taken from our previous paper[11]. The two high frequency bands in Fig. 2 at 345 and 690 cm^{-1} are also evident in the multiphonon IR spectrum of As_2S_3 glass.

We have indicated in Fig. 3 the overtones and combinations of the two highest frequency fundamentals of As_2S_3 in Fig. 2, the 345 cm^{-1} band (designated $\bar{\nu}_A$) and the 485 cm^{-1} band (designated $\bar{\nu}_B$). In line with our molecular model hypothesis for multiphonon absorption in chalcogenide glasses, these overtones and combinations correspond well to the prominent features of the As_2S_3 spectrum (maximum at 690 cm^{-1}, change in slope around 800 cm^{-1}, maximum at 980 cm^{-1}, shoulder at 1050 cm^{-1}, etc.).

The similarity of the spectra of As_2S_3 and As_2Se_3 glasses in Fig. 3 is a striking demonstration of the isostructural character of these two glasses, as suggested in Fig. 1. The dashed line in Fig. 3 is the spectrum of As_2Se_3 scaled to that of As_2S_3 using a frequency scaling factor $\bar{\nu}_{As_2Se_3}/\bar{\nu}_{As_2S_3}$ of 0.70 and an amplitude scaling factor $\alpha_{As_2Se_3}/\alpha_{As_2S_3}$ of 0.63 [11]. The frequency scaling factor is the same as that found by Zallen et al.[17] to relate the Raman and IR spectra peak frequencies of both

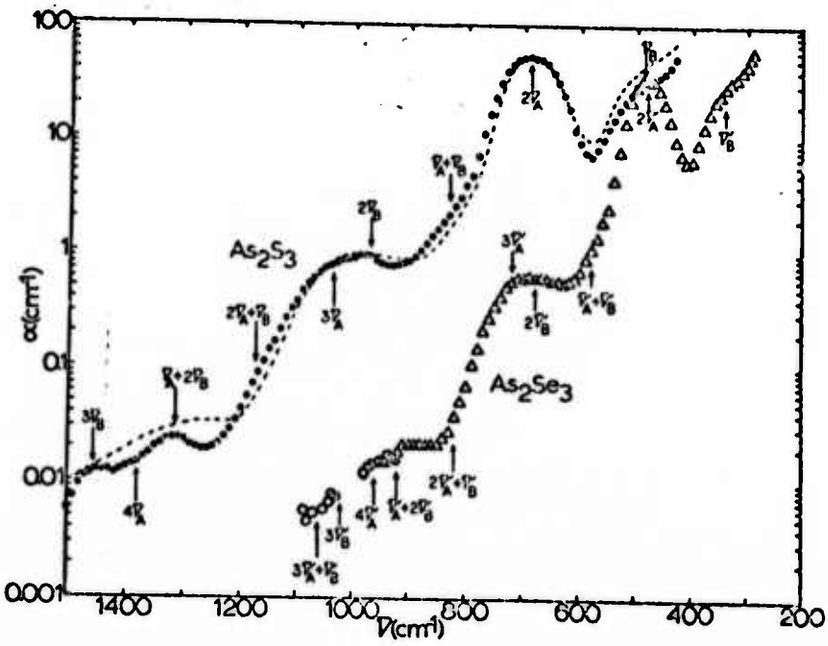

Figure 3. IR absorption coefficient versus wavenumber for As_2S_3 and As_2Se_3 glasses at ambient temperature.

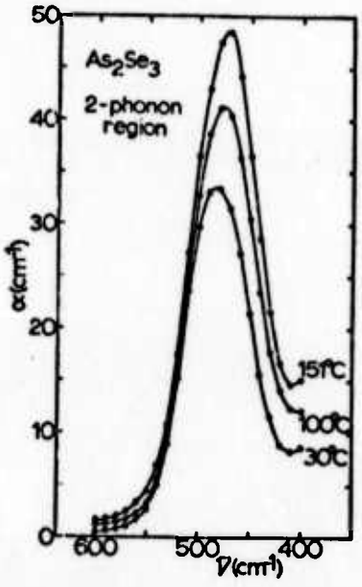

Figure 4. IR absorption coefficient versus wavenumber plots for As_2Se_3 glass as a function of temperature in the 2-phonon region.

amorphous and crystalline As_2S_3 and As_2Se_3 in the fundamental region.

From the above frequency scaling factor the two highest frequency peaks in the fundamental region for As_2Se_3 glass are predicted to lie at $\bar{\nu}_A' = 240$ cm^{-1} (close to the intense Raman peak observed at 227 cm^{-1} [18]) and at $\bar{\nu}_B' = 340$ cm^{-1} (observable as a shoulder in Fig.3). Overtones and combinations of these frequencies are indicated in the As_2Se_3 spectrum of Fig. 3 and correspond well to prominent features in the spectrum.

TEMPERATURE DEPENDENCE OF ABSORPTION COEFFICIENTS

In Fig. 4 are shown plots at different temperatures of α versus $\bar{\nu}$ for As_2Se_3 glass in the vicinity of the 2-phonon absorption peak at 480 cm^{-1}. The absorption coefficient increases in magnitude and the maximum shifts slightly to lower frequencies with increasing temperature. α versus $\bar{\nu}$ plots in the vicinity of the 700 cm^{-1} maximum of Fig. 3 for As_2Se_3 show similar behavior as a function of temperature.

The shift in the absorption peaks to lower frequency with increasing temperature may be understood if we assume that the fundamental vibrational modes (the $AsSe_3$ and As-Se-As group stretching vibrations) are anharmonic (e.g., described by a Morse potential), so that the spacing of the vibrational energy levels narrows with increasing vibrational quantum number. Increasing temperature increases the population of the levels of higher quantum number and hence increases the relative number of mulitphonon absorption processes originating in the higher vibrational states, leading in turn to a decrease in the average frequency for a given multiphonon process. In the temperature range covered in our experiments on As_2Se_3 glass, however, the changes in multiphonon absorption maxima frequency are so small that they may be neglected in our discussion below of the temperature dependence of α.

For a multiphonon absorption process in which a photon of wavenumber $\bar{\nu}$ is absorbed and produces n phonons of the same fundamental wavenumber $\bar{\nu}_f$ the ratio of the absorption coefficient at temperature T to that at 0 K is predicted to be

$$\alpha(T)/\alpha(0) = [1-\exp(-nhc\bar{\nu}_f/kT)]/[1-\exp(-hc\bar{\nu}_f/kT)]^n \quad (2)$$

where h is Planck's constant, c is the velocity of light, and k is the Boltzmann constant (cf. refs. 7-9,19 and papers cited therein). In Fig. 5 the absorption coefficients of As_2Se_3 glass at 480 cm^{-1} (Fig. 4) are plotted versus temperature. The line for the 480 cm^{-1} data in Fig. 5 is calculated from Eq. (2) using n = 2 and an $\alpha(0)$ value selected to cause the calculated curve to agree with the experimental data at 75° C. The temperature dependence of α at 480 cm^{-1} is in good agreement with that predicted for a 2-phonon absorption process, in accord with our molecular model analysis of the data of Fig. 3. The temperature dependence of α at 700 cm^{-1} shown in Fig.5 is intermediate between that predicted for n = 2 and that for n = 3, similarly in accord with the molecular model analysis summarized in Fig. 3, although the 3-phonon process appears to dominate absorption at this frequency. In the CO_2 laser region (920-1090 cm^{-1}) the molecular model predicts a variety of 3- and 4-phonon absorption processes for As_2Se_3 as shown in Fig. 3. The temperature dependence of α at 943 and 1026 cm^{-1} shown in Fig.6 is again in good agreement with this prediction.

MULTIPHONON ABSORPTION IN MIXED CHALCOGENIDE GLASSES

In this section we will discuss multiphonon absorption in the mixed chalcogenide glasses X As_2S_3 - (1-X) As_2Se_3 and X As_2Se_3 - (1-X) $GeSe_2$, where X is the mole fraction of the first component of each pair. Since, as is evident from Fig. 3, a large number of multiphonon processes become possible at high frequencies even for one component glasses, we shall confine our remarks on the mixed glasses for the most part to the low frequency 2-phonon region in which absorption is due to the pyramidal AsY_3 and tetrahedral GeY_4 group stretching modes.

In Fig. 7 are shown α versus $\bar{\nu}$ plots taken from our previous paper[11] for two mixed X As_2S_3 - (1-X)As_2Se_3 glasses. The solid curves are the absorption coefficients predicted on the basis of additivity of the α values of the end member compositions, As_2S_3 (= component 1) and As_2Se_3 (=component 2), at each frequency:

$$\alpha = f\alpha_1 + (1-f)\alpha_2 \quad (3)$$

f is the volume fraction of component 1:

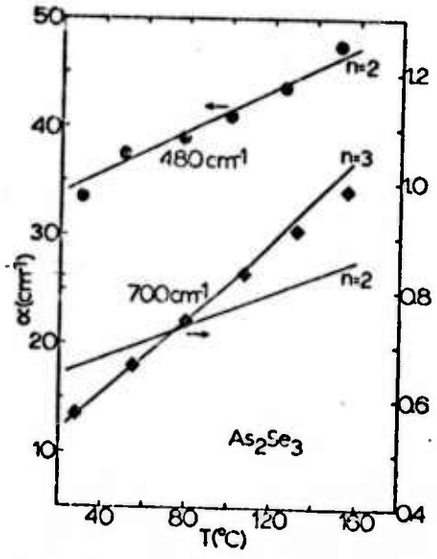

Figure 5. IR absorption coefficient versus temperature at 480 and 700 cm^{-1} for As_2Se_3 glass. Solid lines calculated from Eq. (2) using n values shown in the figure and $\alpha(0)$ values selected to give agreement with the data at 75° C.

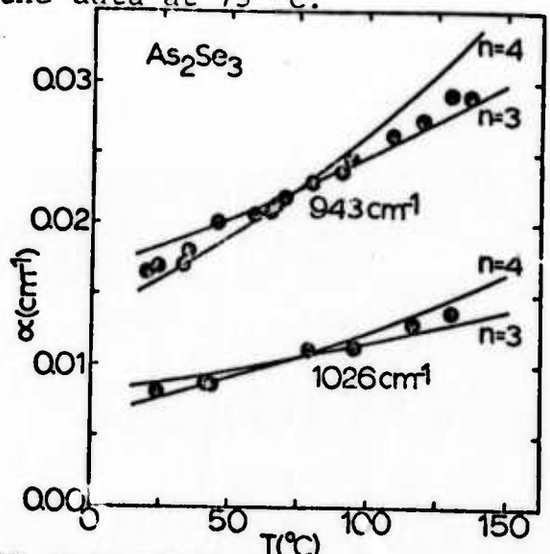

Figure 6. IR absorption coefficient versus temperature at 943 and 1026 cm^{-1} for As_2Se_3 glass. Solid lines calculated from Eq. (2) using n values shown in the figure and $\alpha(0)$ values selected to give agreement with the data at 75° C.

$$f = (XM_1/\rho_1)/[(XM_1/\rho_1) + ((1-X)M_2/\rho_2)]$$

where X, M_1, and ρ_1 are the mole fraction, formula weight, and density of component 1 and (1-X), M_2, and ρ_2 the corresponding quantities for component 2. The glass densities are given in our previous paper[11]. For X = 0.602 the experimental and calculated additive α values agree within about 20% except in the region around 585 cm^{-1}. For X = 0.074 the agreement is somewhat worse, but still fairly close, except again in the region around 585 cm^{-1}.

Felty and coworkers [20] have observed two reststrahlen bands in reflectivity measurements in the fundamental region of mixed As_2S_3-As_2Se_3 glasses; the two reststrahlen frequencies corresponded closely to those for the pure glasses. Lucovsky[21] suggested that this behavior could be accounted for either by assuming that the mixed glass reflectance spectra were a superposition of the spectra of different AsY_3 polymeric entities in the glass or that the mixed glasses exhibited the two mode reststrahlen behavior found in solid solutions such as CdS_zSe_{1-z} in which the component atoms had large mass differences. In terms of the molecular model for the vibrational characteristics of As_2S_3 and As_2Se_3 the former explanation is to be preferred.

In the mixed As_2S_3 - As_2Se_3 glasses one would expect a structure of the type shown in Fig. 1 with the two types of chalcogen atoms distributed over the As-Y-As bridging groups, so that a substantial portion of the AsY_3 pyramids should consist of mixed AsS_2Se and $AsSSe_2$ groups. The lowered symmetry of these mixed groups would lead to splitting of the degenerate AsY_3 stretching modes. However, because of the large mass difference between S and Se, the stretching modes for the AsS_2Se and $AsSSe_2$ should be close in frequency to those for AsS_3 and $AsSe_3$, i.e., should be approximately equal to $\bar{\nu}_A$ and $\bar{\nu}_A'$ of Fig. 3, in agreement with the observations of Felty and coworkers[20] in the fundamental region of the mixed glasses. In the 2-phonon absorption region ascribable to the AsY_3 stretching modes one would expect to observe combination and overtone bands at $2\bar{\nu}_A$ = 690 cm^{-1}, at $2\bar{\nu}_A'$ = 480 cm^{-1}, and at $\bar{\nu}_A + \bar{\nu}_A'$ = 585 cm^{-1}. The first two of these predicted 2-phonon bands (690 and 480 cm^{-1}) are quite apparent in Fig. 7, but the predicted 585 cm^{-1} band is

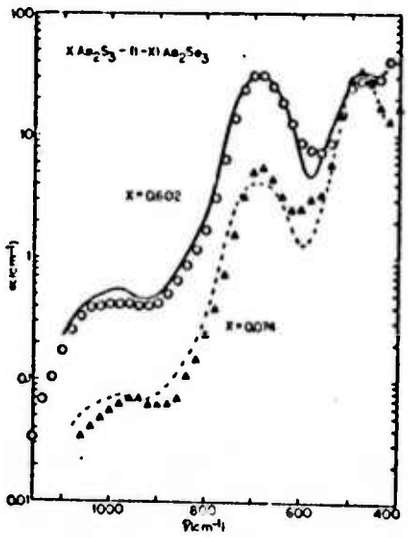

Figure 7. IR absorption coefficient versus wavenumber for X As_2S_3-(1-X)As_2Se_3 glasses. Solid and dashed curves are calculated from Eq. (3).

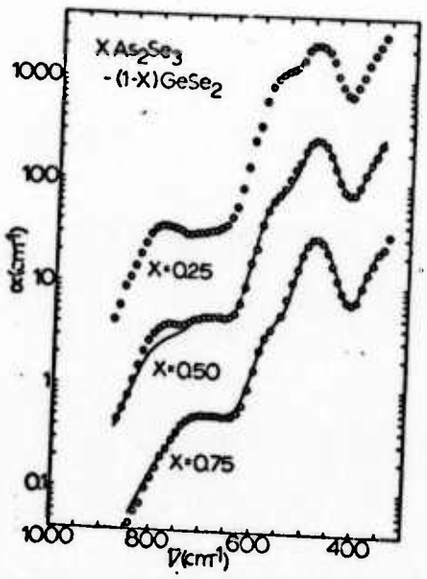

Figure 8. IR absorption coefficient versus wavenumber for X As_2Se_3-(1-X)$GeSe_2$ glasses. The α scale is correct for the X = 0.75 glass; for clarity the spectra have been displaced upward by respective factors of 10 and 100 in α.for the X = 0.50 and X = 0.25 glasses. Solid curves are calculated from Eq. (3).

discernible only in terms of the large deviations from additivity at this frequency and as a peak shoulder at about 580 cm^{-1} in the X = 0.074 gla . The relative weakness of predicted 585 cm^{-1} bands which should occur only in the mixed As_2S_3 - As_2Se_3 glasses may mean that the distribution of the S and Se atoms among the bridging groups may be highly non-random[11].

In Fig. 8 are shown α versus $\bar{\nu}$ plots in the multiphonon region for mixed X As_2Se_3 - (1-X) $GeSe_2$ glasses. We were unable to obtain the end member composition $GeSe_2$ in the glassy state by rapid quenching of bulk samples, contrary to the report of Tronc and coworkers[22] but in agreement with earlier reports of the glass-forming regions in the Ge-As-Se system[23], so that our studies cover only the composition range X = 0.25 to 1.00. The peaks at 780 cm^{-1} in Fig. 8 for the compositions X = 0.25 and 0.50 are due to oxide impurity[24], but below 700 cm^{-1} the spectra of all the glasses are due to intrinsic absorption processes.

The ambient temperature densities of the X As_2Se_3-(1-X) $GeSe_2$ glasses were [X,ρ(g/cm^3)]: 0.25, 4.34; 0.50, 4.40; 0.75, 4.53; 1.00, 4.61. Within experimental error the molar volumes were additive.

The solid curves in Fig. 8 are the absorption coefficients calculated from Eq. (3) on the assumption of additivity of the α values of the end member composition As_2Se_3 (= component 1) and $GeSe_2$ (= component 2). Since the pure $GeSe_2$ glass could not be prepared, the α_2 values were calculated from Eq. (3) using the experimental α values for the X = 0.25 compositions. These calculated α_2 values were then used to calculate the solid curves of Fig. 8 for the X = 0.50 and 0.75 composition . The agreement between the experimental and calculated additive α versus $\bar{\nu}$ curves in the intrinsic region below 700 cm^{-1} is within experimental error.

From Fig. 1 the structure of the mixed As_2Se_3 - $GeSe_2$ glasses is expected to consist of $AsSe_3$ pyramids and $GeSe_4$ tetrahedra linked by Se atom bridges. The molecular model predicts that the vibrations of neighboring $AsSe_3$ and $GeSe_4$ groups should be only very loosely coupled, so that in the multiphonon absorption region one expects in turn to see no combination bands of

$AsSe_3$ and $GeSe_4$ fundamental frequencies. The 400 to 600 cm^{-1} region of Fig. 8 is the frequency range in which 2-phonon processes involving the $AsSe_3$ and $GeSe_4$ stretching modes are predicted to occur, and hence the agreement of the spectra of the mixed glasses in this region with those predicted from Eq. (3) on the assumption of additivity of the end member spectra are in complete agreement with this hypothesis.

In summary, then, for mixed chalcogenide glasses the molecular model predicts additivity of absorption coefficients in the 2-phonon region when the high coordination center atoms are mixed, as in the As_2Se_3-$GeSe_2$ glasses, but deviations from additivity when the bridging chalcogen atoms are mixed, as in the As_2S_3-As_2Se_3 glasses. These predictions are in accord with the experimental results reported here.

ACKNOWLEDGMENTS

This research was supported by contracts from the Advanced Research Projects Agency and from the Office of Naval Research. The authors wish to thank Mr. P. Pureza and Mr. J. Lowans for assistance in sample preparation and characterization.

REFERENCES

1. G. Lucovsky and R.M. Martin, J. Non-Cryst. Solids, 8-10, 185, (1972).
2. G. Lucovsky, Phys. Rev. B, 6, 1480 (1972).
3. G. Lucovsky, J.P. deNeufville, and F.L. Galeener, Phys. Rev. B, 9, 1591 (1974).
4. G. Lucovsky, F.L. Galeener, R.C. Keezer, R.H. Geils, and H.A. Six, Phys. Rev. B, 10, 5134 (1974).
5. R.J. Kobliska and S.A. Solin, Phys. Rev. B, 8, 756 (1973).
6. G.N. Papatheodorou and S.A. Solin, Solid State Commun., 16, 5 (1975).
7. D.W. Pohl and P.F. Meier, Phys. Rev. Lett., 32, 58 (1974).
8. T.F. McNeely and D.W. Pohl, Phys. Rev. Lett., 32, 1305 (1974).
9. L.L. Boyer, J.A. Harrington, M. Hass, and H.B. Rosenstock, Phys. Rev. B, in press.

10. T.F. Deutsch, J. Phys. Chem. Solids, 34, 2091 (1973).
11. M.S. Maklad, R.K. Mohr, R.E. Howard, P.B. Macedo, and C.T. Moynihan, Solid State Commun., 15, 855 (1974).
12. C.T. Moynihan, P.B. Macedo, M.S. Maklad, R.K. Mohr, and R.E. Howard, J. Non-Cryst. Solids, in press.
13. D.A. Pinnow and T.C. Rich, Appl. Opt., 12, 984 (1973).
14. F.A. Horrigan and T.G. Deutsch, "Research in Optical Materials and Structures for High Power Lasers," Quarterly Technical Report No. 2, Raytheon Research Div., Waltham, MA , Contract DAAH01-72-C-0194, 1972.
15. R.J. Kobliska and S.A. Solin, Solid State Commun., 10, 231 (1972).
16. A.T. Ward, J. Phys. Chem., 72 4133 (1968).
17. R. Zallen, M.L. Slade, and A.T. Ward, Phys. Rev. B, 3, 4257 (1971).
18. J. Schottmiller, M. Tabak, G. Lucovsky, and A. Ward, J. Non-Cryst. Solids, 4,80 (1970).
19. H. P. Rosenstock, Phys. Rev. B, 9, 1963 (1974).
20. E.J. Felty, G. Lucovsky, and M.B. Myers, Solid State Commun., 5, 555 (1967).
21. G. Lucovsky, Mat. Res. Bull., 4, 505 (1969).
22. P. Tronc, M. Bensoussan, A. Brenac, and C. Sebenne, Phys. Rev. B, 8, 5947 (1973).
23. R.W. Haisty and H. Krebs, J. Non-Cryst. Solids, 1 427 (1969).
24. J. A. Savage and S. Nielsen, Infrared Physics, 5, 195 (1965); Phys. Chem. Glasses, 6, 90 (1965).